JGR Biogeosciences

RESEARCH ARTICLE
10.1029/2020JG006024

Where Does Moisture Come From Over the Congo Basin?

Sarah Worden[1], Rong Fu[1], Sudip Chakraborty[2], Junjie Liu[2,3], and John Worden[2]

[1]University of California, Los Angeles (UCLA), Los Angeles, CA, USA, [2]Jet Propulsion Laboratory (JPL), California Institute of Technology, Pasadena, CA, USA, [3]California Institute of Technology, Pasadena, CA, USA

Key Points:

- Evapotranspiration (ET) is the main source of atmospheric moisture in the Congo Basin
- ET is the dominant source of atmospheric moisture during the transition to the spring rainy season
- Photosynthesis seasonally covaries with deuterium, suggesting that transpiration significantly contributes to atmospheric moisture

Correspondence to:
R. Fu,
rfu@atmos.ucla.edu

Citation:
Worden, S., Fu, R., Chakraborty, S., Liu, J., & Worden, J. (2021). Where does moisture come from over the Congo Basin? *Journal of Geophysical Research: Biogeosciences*, *126*, e2020JG006024. https://doi.org/10.1029/2020JG006024

Received 5 SEP 2020
Accepted 26 JUL 2021

Abstract The Congo Basin hosts the world's second largest rainforest and is a major rainfall center. However, the primary sources of moisture needed to maintain this forest, either from evapotranspiration (ET) or advection from the ocean, remain unclear. We use satellite observations of the deuterium content of water vapor (δD), solar induced fluorescence (SIF), precipitation, and atmospheric reanalysis to examine the relative contribution of ET to moisture in the free troposphere. We find that SIF, an indicator of photosynthesis, covaries with δD in early rainy seasons, suggesting that ET is an important contributor to atmospheric moisture in both the spring and fall rainy seasons. However, the relative contribution of ET to the free tropospheric moisture varies between the two rainy seasons. Observed δD relative to a range of observationally constrained, isotopic mixing models representative of water vapor coming from land suggests that $83\% \pm 9\%$ of the free tropospheric moisture come from ET in February, and $45\% \pm 13\%$ in April, versus $59\% \pm 12\%$ in August and $31\% \pm 12\%$ in October. Reanalysis indicate that this difference between seasons is due to increased advection of ocean air during the fall season, thus reducing the relative contribution of ET to the Congo Basin in the fall. In addition, ET is the primary atmospheric moisture source in the winter and summer dry seasons, consistent with estimates reported in literature. Our results highlight the importance of ET from the Congo rainforest as an important source of moisture for initiating the rainy seasons.

Plain Language Summary The Congo Basin hosts the world's second largest rainforest and is a major rainfall center. It has been unclear whether moisture from the adjacent oceans or from evapotranspiration of the rainforests is its main moisture source, especially for initiating the rainy seasons. Using a suite of satellite data, we show that evapotranspiration, especially transpiration, is important for atmospheric moisture throughout the year. However, the relative contribution of ocean moisture from transport increases prior to fall rainy season and not prior to the spring rainy season, indicating that the relative contribution of ET to atmospheric moisture is higher in spring than in fall. Our finding highlights the importance of the rainforests in maintaining and modulating atmospheric humidity.

1. Introduction

The Congo Basin, located in the equatorial Africa, hosts the world's second largest, contiguous rainforests (Figure 1). While its annual rainfall (1,500–2,500 mm) is lower than that of the Amazon (1,800–3,200 mm) (Alsdorf et al., 2016), its rainy seasons in boreal spring (March-April-May, denoted MAM) and boreal fall (September-October-November, denoted SON) limit the dry seasons to about 3–4 months in summer (June-July-August, denoted JJA) and winter (December-January-February, denoted DJF), and thus help to sustain the rainforests (e.g., Staver et al., 2011; Mayer & Khalyani, 2011). These two rainy seasons are associated with the north-south migration of the rain belt over tropical Africa that crosses the Congo Basin (Nicholson & Dezfuli, 2013); however, the complex interactions between large-scale atmospheric circulation, mesoscale convective processes, and moisture availability from ocean and terrestrial sources drive their onset and demise (e.g., Nicholson, 2018). These mechanisms that control the variability and changes of the rainy seasons over the Congo Basin are thus poorly understood (e.g., Alsdorf et al., 2016; Nicholson, 2018), leading to large uncertainties in representing its current and future rainfall in climate models (e.g., James et al., 2018; Washington et al., 2013).

Observations have shown that a decrease of rainfall and reduced terrestrial water storage in the Congo Basin have likely led to a decrease in vegetation greenness as well as widespread water deficits between 2003 and 2012 (e.g., Reager et al., 2016; Samba & Nganga, 2012; Zhou et al., 2014). Furthermore, the boreal summer dry season length has likely increased since the 1980s, mainly due to an earlier ending of the spring

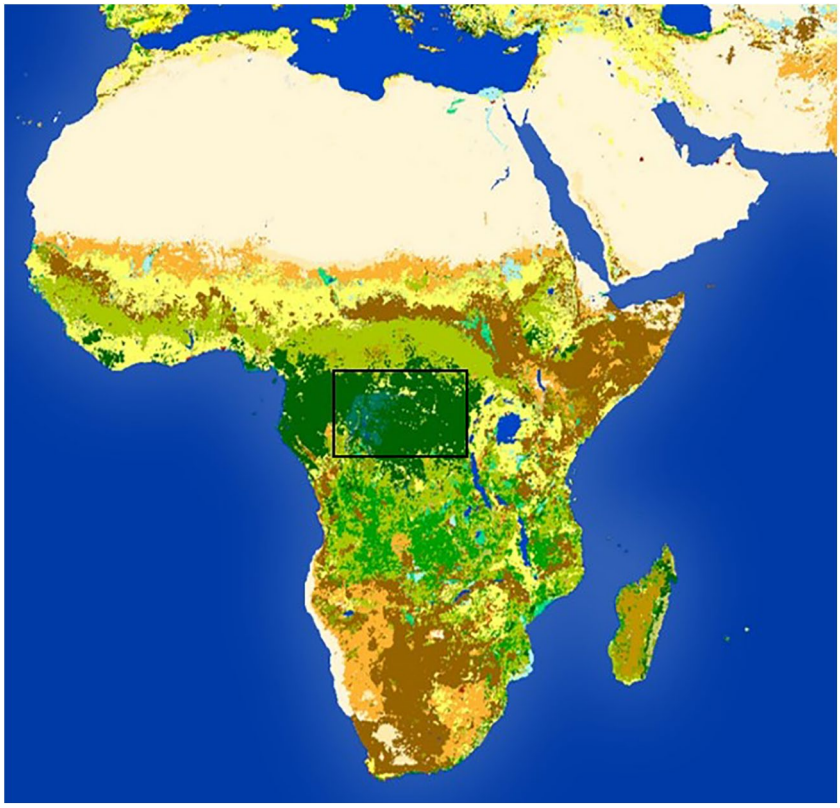

Figure 1. Map of Africa in 2015 showing the different types of vegetation. The central green area is evergreen rainforest, and the boxed area within it is the region used for analysis of the Congo Basin, 15:30°W and −5:5°N. Data are taken from the European Space Agency (ESA) Climate Change Initiative (CCI) Land Cover products (Defourny et al., 2017).

rainy season (Jiang et al., 2019). Enhanced water stress could subsequently alter the composition and structure of the evergreen rainforests over the Congo Basin, which are already vulnerable to abrupt transitions to savanna ecosystem as annual rainfall over much of the Congo Basin is low relative to other rainforests (Alsdorf et al., 2016; Jiang et al., 2019; Staver et al., 2011). These changes in both rainy seasons and rainforest composition thus highlight the need for understanding the mechanisms that control rainy season variability, especially whether and how reduced and degraded rainforests could affect the rainy seasons over the Congo Basin through a change in the supply of moisture from evapotranspiration (ET), as well as changes in latent and sensible heating. For example, numerical model simulations have shown that deforestation, as well as the alteration of the composition of the Congo rainforest toward more drought resistant species, can lead to decreased ET, clouds and rainfall (Bell et al., 2015). Understanding the source of moisture for rainfall over Congo Basin should therefore allow us to better project future changes in the water cycle and its interaction with vegetation over the Congo Basin.

Moisture availability in the lower troposphere is central to rainfall frequency and intensity over the tropics in general (e.g., Bretherton et al., 2004; Holloway & Neelin, 2009; Schiro et al., 2018; Sobel et al., 2004), including the Congo region (Taylor et al., 2018). Previous studies have attributed rainfall variability on interannual to interdecadal timescales over the Congo Basin to sea surface temperature anomalies (SSTA) over the tropical Pacific, Atlantic, and Indian oceans through their influences on moisture transport (Balas et al., 2007; Dai, 2013; Diem et al., 2014; Hoerling et al., 2006; Hua et al., 2016; Nicholson & Dezfuli, 2013; Pokam et al., 2014; Tamoffo et al., 2019). Other studies, using methods such as global models or back trajectories, have found large recycling ratios (over 50%) in the Congo Basin, indicating ET is an important source of moisture for the area (e.g., Risi et al., 2013; van der Ent et al., 2010). It is important to distinguish that here we consider the fraction of water vapor in the atmosphere over the Congo Basin originating from land ET anywhere (e.g., Risi et al., 2013; van der Ent et al., 2010; Yoshimura et al., 2004), rather the typical

recycling ratio that calculates the fraction of water vapor originating from land ET only within the domain (e.g., Eltahir & Bras, 1996; Trenberth, 1999).

Determining the contributions of free-tropospheric moisture from ocean evaporation versus ET from vegetation in the Congo Basin is therefore key for developing a better understanding of the relative influences on precipitation from external SSTA, internal land vegetation, and land-use changes. However, most recycling rates heavily rely on model or reanalysis to determine the contribution of ET to precipitation (e.g., Risi et al., 2013; van der Ent et al., 2010). Measurements of the isotopic composition of rainfall and rivers, when combined with reanalysis-based wind fields and satellite observations of rainfall have been shown to be useful for quantifying the sources of precipitation for different regions of Africa. For example, Levin et al. (2009) has used in situ measurements of oxygen 18 ($\delta^{18}O$) and δD from rivers, as well as Tropical Rainfall Measuring Mission (TRMM) precipitation and wind fields, to show that oceanic moisture is the primary source of precipitation for Kenya, while ET is the primary source of precipitation for Ethiopia. However, in situ measurements of isotopes are virtually unavailable over the Congo Basin. Satellite measurements of δD are sensitive to their oceanic versus terrestrial sources over the global tropics and can therefore be used to identify moisture sources and processes controlling atmospheric humidity (e.g., Brown et al., 2008; Risi et al., 2010; Worden et al., 2007). We use such satellite observations of δD, rainfall, and photosynthesis, along with reanalysis to determine the relative importance of the ET versus moisture transport to the Congo Basin atmospheric moisture using an approach similar to Wright et al. (2017). These data therefore allow us to test a hypothesis that ET is the primary moisture source for the Congo Basin rainy seasons.

2. Data

The deuterium content of water is expressed as the relative ratio of the number of HDO molecules to the total number of H_2O molecules in parts per thousand (‰) relative to the isotopic composition of ocean water as shown below:

$$\delta D = 1000 \times \left(\frac{R - R_{\text{std}}}{R_{\text{std}}} \right) \tag{1}$$

where R is the ratio of the number of HDO molecules to the total number of H_2O molecules and R_{std} is the corresponding ratio in a reference standard, taken here to be the Vienna Standard Mean Ocean Water: $R_{\text{std}} = 3.11 \times 10^{-4}$ (e.g., Wright et al., 2017 and references therein). The isotopic composition of water vapor in the free troposphere is due to a mixture of air parcels originating from different sources (Galewsky, 2018; Galewsky & Hurley, 2010; Galewsky et al., 2016). Free-tropospheric δD measurements are from the National Aeronautics and Space Agency (NASA) Aura Tropospheric Emission Spectrometer (TES) satellite instrument. The analysis period of this study is 2005–2011 when the quality of TES δD data are suitable for our analysis. We use the monthly mean TES version 6 (v006_Litev01.00) Level 2 volume mixing ratios of δD in this study. The following quality flags were used when retrieving the data from the TES satellite: "Species Retrieval Quality = 1," "Degrees of Freedom for Signal > 1," and "Average Cloud Optical Depth < 0.4" in order to ensure good quality data as suggested by Worden et al. (2012). The accuracy of these data is ~6 per mil with a precision of 20 per mil (Worden et al., 2012) for the vertical range used in this analysis (~900–420 hPa, or about 1–6 km above sea level). For this study, we use the average δD over this vertical range.

Measurements of solar induced fluorescence (SIF) provide a nearly direct estimate of photosynthesis, a prerequisite for transpiration (e.g., Frankenberg et al., 2011). We can therefore use SIF to indicate the occurrence of transpiration, one of the main components of ET. A caveat is that transpiration also depends on plant water use efficiency, vapor pressure deficit, and radiation (e.g., Boese et al., 2017) so that we might not expect a one-to-one relationship between SIF and ET. We use SIF estimates from the GOME-2 V26 740 nm data products (Joiner et al., 2013) as their observational period overlaps with most of the TES record (2007–2011). The precipitation estimates taken from TRMM are from the 3B43 gridded monthly average estimate at a horizontal resolution of $0.25° \times 0.25°$. TRMM precipitation estimates are generated using a combination of microwave and radar sensors on the instrument that are calibrated with gauge data from the Global Precipitation Climatology Center (GPCC) (Huffman et al., 2007).

ET data comes from a combination of reanalysis and the Moderate Resolution Imaging Spectroradiometer (MODIS) as described in Fisher et al. (2009). While there are a variety of choices of ET and precipitation, we are using these data primarily for qualitative comparisons to give an understanding of what is likely known. A full error analysis of ET and precipitation products is beyond the scope of this study, but described in the literature (Fekete et al., 2004; Fisher et al., 2009; Munier & Aires, 2018; Pan et al., 2020; Rauniyar et al., 2017).

We also use the Fifth Generation of the European Center for Medium-Range Weather Forecasts (ECMWF) Reanalysis (ERA5) monthly means of daily means of the longitudinal (u) wind component, latitudinal (v) wind component, and vertically integrated moisture flux divergence on a 0.25° × 0.25° grid (Hersbach et al., 2020, https://www.ecmwf.int/en/forecasts/datasets/reanalysis-datasets/era5). The reanalysis is a four-dimensional (i.e., space and time) data assimilation product that combines observations with model forecasts to estimate the dynamic and thermodynamic structures of the global atmosphere. Although the quality of reanalysis in general has been open to debate (Dee et al., 2011; Pan et al., 2020; Thorne & Vose, 2010), using this data in conjunction with observation-based data allows us to corroborate information of the moisture source that cannot be directly provided by observations.

3. Comparison of Isotope Observations With Theoretical Mixing and Rayleigh Models

3.1. Deuterium Content of Water

We can use the isotopic composition of an air mass to trace its source to either vegetation or ocean because δD values contributed by ocean evaporation are distinctively different from those by rainforest ET. Rainwater will generally be more isotopically enriched (or heavier) than the source vapor because heavier isotopes preferentially condense (Risi et al., 2020; Tremoy et al., 2014; Worden, et al., 2007). Since the deuterium content of transpired water is relatively unchanged from that of the original source, for example, the isotopically heavier rainwater (Risi et al., 2013), it will be more enriched than the vapor evaporated from its oceanic source. Therefore, by examining the differences in deuterium content of the water vapor over a heavily vegetated surface, one can separate water coming from the ocean from water coming from plants (Wright et al., 2017).

The observed values of free-tropospheric deuterium content also depend on the type of convection. Some form of mixing between the surface and free troposphere is required to transport surface fluxes into the air parcels observed by the satellite. For example, shallower convection detrains near the midtroposphere, enriching δD of the midtropospheric water vapor (Lacour et al., 2018). Deeper convection, while also mixing air between the surface and free troposphere, is associated with other processes beside condensation that affect the isotopic composition of vapor such as rainfall evaporation (Lacour et al., 2018; Worden et al., 2007). The latter is a confounding factor in our conclusions. For example, Nlend et al. (2020), using a back trajectory method, suggests that δD of rainfall is primarily controlled by upstream mesoscale convective systems instead of ET in West-Central Africa. On the other hand, other research such as from Moore et al. (2014) and Bailey et al. (2017) suggest that the free-tropospheric signal is primarily related to moisture convergence and hence the balance between evaporation and precipitation, even during times of deep convection. Our interpretation of the moisture sources is less influenced by these uncertainties during the months before and after the peak of each rainy season when deep convection is expected to influence δD.

3.2. Mixing and Rayleigh Models

We first quantify the seasonality of the isotopic composition of water vapor in the free-troposphere and then compare such parcels with two models, a mixing model and a Rayleigh model, to identify which air parcels are likely influenced by land versus ocean (Noone, 2012). A mixing model describes what happens to a mixture of two air masses with different water vapor isotopic compositions:

$$\delta_{\text{mix}} = q_0\left(\delta_0 - \delta_F\right)\frac{1}{q} + \delta_F \tag{2}$$

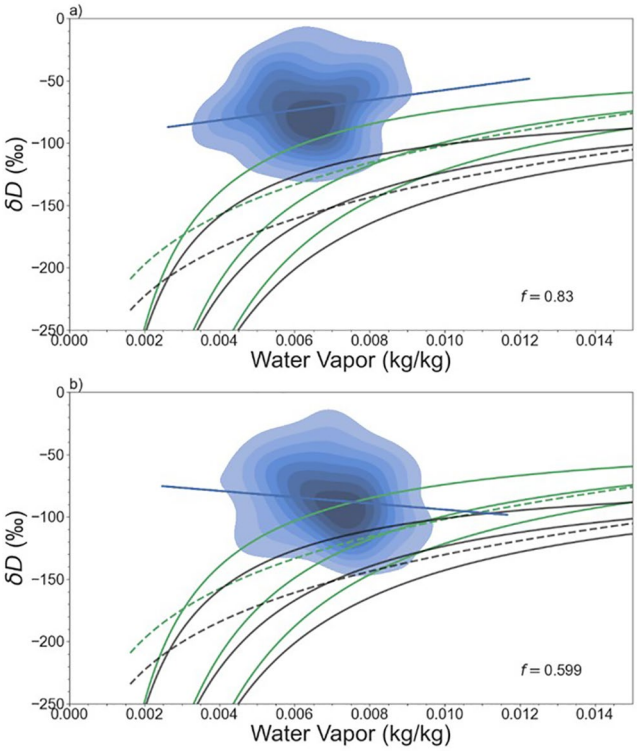

Figure 2. Density plot of individual free-tropospheric δD measurements over the Congo Basin in (a) February; (b) August; Blue line is a linear line of best fit. The green and gray solid lines represent mixing models with water originating from land and ocean, respectively, for different initial values of q0 and qF ranging between 0.0016–0.0046 and 0.02–0.052, respectively. The dashed green and gray lines represent Rayleigh models with initial values $q_0 = 0.0016$ and $q_s = 0.02$. The numbers in the bottom right corner are the fraction of δD above the upper most, land-based mixing model (f). Higher f indicates a relatively greater contribution of evapotranspiration to atmospheric moisture.

where q_0 and δ_0 are the specific humidity and its δD value of the dry air mass in the upper troposphere, and q_F and δ_F are the specific humidity and δD value of the air mass at the surface. $q = q_0 + q_F$ is the specific humidity of the mixed air mass between dry air mass in the upper troposphere and humid air mass from its surface source (Noone, 2012). This model considers two possible moisture sources for the air mass sampled by TES δD measurements: air with water vapor transpired from the rainforest, and air with water vapor evaporated from the ocean. Generally, the isotopic composition of vapor sourced from vegetation over the tropical land (δ_F for vapor from ET) is between −75‰ and 0‰ while the isotopic composition of vapor sourced from the ocean (δ_F for vapor from ocean) is lower than −75‰ (Risi et al., 2013).

We also examine the observed δD values in relation to a Rayleigh model, which describes the change of δD with water vapor mixing rate as liquid water evaporates in equilibrium with temperature:

$$\delta_{\text{ray}} \simeq (\alpha - 1)\ln\left(\frac{q}{q_0}\right) + \delta_0 \quad (3)$$

where α is set to equal the temperature-dependent equilibrium fractionation factor between liquid and water vapor (Majoube, 1971). Under the Rayleigh distillation model, as an air mass moves upward (or toward cooler conditions), condensate is completely removed immediately after it forms under the assumption of pseudo adiabatic process (Galewsky & Hurley, 2010; Wright et al., 2017). During deep convection, air parcel moisture is more isotopically depleted than expected from Rayleigh models because of a combination of processes that occur during convection such as rainfall evaporation and entrainment of isotopically depleted air (Worden et al., 2007).

This combination of mixing and rainfall processes compared to observed δD is illustrated for February and August, the transition months to the boreal spring and fall rainy season, respectively, in Figure 2. The solid curves represent mixing models with different initial δD values that originate from land (green) and ocean (gray) and mix with air representative of the upper troposphere (e.g., Samuels-Crow et al., 2014). The initial values of modeled δD (δ_F) were −50‰ and −80‰ for land-based and ocean-based models, respectively, chosen based on representative values of δD from land and ocean. We chose this initial condition of −50‰ for a land-based model to ensure that observations above mixing models with this boundary condition originate from a terrestrial source. Furthermore, the uppermost, land-based mixing model is the only model that does not intersect with the ocean-based mixing models. Therefore, any observed δD located above the uppermost land-based mixing line in Figure 2 is most likely from ET. Any δD value shown between the land-based and ocean-based mixing lines likely comes from some mixture of the two sources.

We assess if our assumptions for the isotopic mixing models and Rayleigh models significantly affect our estimates of the relative contribution of ET versus moisture transport from ocean to the atmospheric moisture. For example, Risi et al. (2013) suggests that convection and large-scale circulation can influence continental recycling estimates based on these free-tropospheric deuterium data. Our approach for setting the bounding conditions for these models is based on Noone (2012): we first found the range of specific humidities at 421 mb (q_0) and near the surface at 1,000 mb (q_F) in Equations 2 and 3 as observed by TES by (a) finding their mean and standard deviation and (b) choosing 10 values between the standard deviation about the mean and the standard deviation added to the mean. Then, we determined how the fraction of δD above the uppermost, land-based, mixing (solid green) model line (hereby denoted as f) changed between February and August for the different values of q_0 and q_F obtained. The mean difference between f estimated by these initial values in February and that in August is 0.199 ± 0.005, where the error is the standard

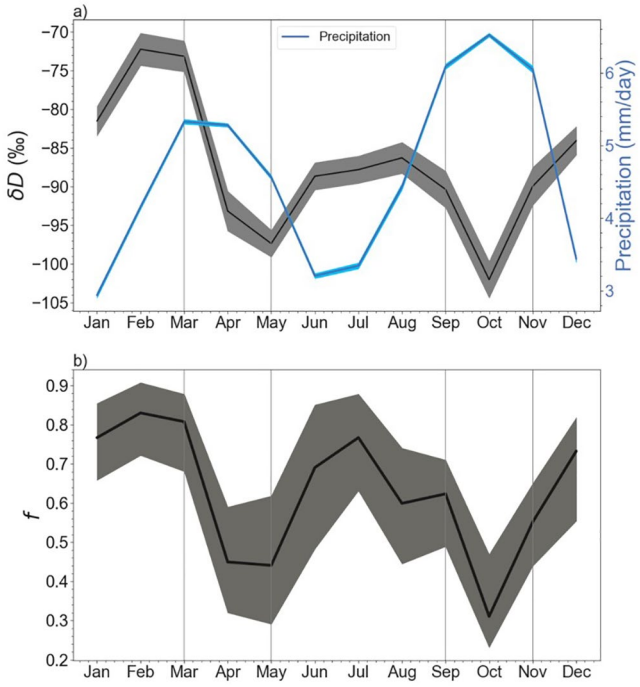

Figure 3. Climatology of (a) Free-tropospheric δD (black line), and its standard error (gray shade), as well as Tropical Rainfall Measuring Mission (TRMM) precipitation (gray line) and its standard error (blue shade). (b) Fraction of the δD samples whose values exceed those of a land-based mixing curve (f). Error is calculated assuming ±12 per mil error in δD measurements. All observed data is averaged over the Congo Basin area of study. Gray lines at March and May as well as September and November denote the two rainy seasons (MAM and SON).

deviation. Though there is a chance that the range of our initial values do not capture the true initial values, the small range of uncertainty of the f difference suggests that our results are not too sensitive to initial values. Therefore, while we show a range of mixing models in Figure 2, hereafter, we only consider the mixing model with the mean values of observed q_0 and q_F when calculating f.

In February (Figure 2a), 83% ± 9% of the data lies above the upper-most, land-based (solid green) mixing line, indicating that this water vapor largely originated from land and then was transported into the free troposphere. We should consider this fraction to be a lower bound on the amount of ET contributing to the Congo Basin atmospheric moisture because rainfall processes as well as vapor originating from oceans will decrease δD. The density contours of δD further suggests a strong contribution from terrestrial sources, as most of the parcels are concentrated between ∼−60‰ and −100‰, values well above the mixing and Rayleigh models for the ocean (dark gray lines) but within the ranges of land-based mixing models. Finally, a linear line of best fit shows an increasing trend toward more enriched δD values as specific humidity increases, consistent with a strong contribution from a terrestrial source (e.g., Risi et al., 2013). In August, 59% ± 15% of the data lies above the land mixing line (Figure 2b), indicating that ET contributes to more than half of the moisture in the atmosphere during the transition month to the fall rainy season, though less than that in the spring. The density contours of δD further overlap mixing and Rayleigh models from both ocean and land sources, also suggesting a mixed contribution from terrestrial and oceanic sources. Finally, a linear line of best fit reveals declining δD values with increasing specific humidity, consistent with reduced continental recycling (Risi et al., 2013). While it is challenging to uniquely identify what combination of moisture sources and rainfall and mixing processes affects the observations below the ocean mixing line using this method, Figure 2 highlights the change in relative importance of ET and oceanic moisture from transport as moisture sources for the boreal spring and fall rainy seasons in the Congo Basin.

4. Results

4.1. The Relative Contributions of ET and Ocean Evaporation to Atmospheric Moisture

Comparison of the isotopic data to the mixing and Rayleigh models (Figure 2) shows that ET likely contributes more moisture in the transition month to the spring rainy season (February) than in the transition month to the fall rainy season (August). To investigate the relative contributions of ET to moisture throughout the year, we examine δD, precipitation, and f, the fraction of the observational samples for which δD exceeds the upper-most land-based mixing model (the top solid green line in Figure 2) in Figure 3.

Precipitation and δD (Figure 3a) show opposing trends in general: increased rainfall corresponds with depleted δD values in rainy seasons and vice versa in dry seasons. This could indicate one of three possibilities: (a) condensation plus rainfall evaporation decreases the deuterium content as discussed previously; (b) increased transport of ocean evaporation into the Congo Basin during peak times could deplete δD measurements and signify an increased contribution of ocean evaporation to atmospheric moisture; or (c) some combination of both are responsible for depleted δD measurements. It is important to note that in the cases of (a) or (c), ET could still have a relatively significant contribution to atmospheric moisture, but precipitation also has a substantial impact on deuterium content.

Compared to the two rainy seasons, the relationship between precipitation and δD is less consistent during the two dry seasons. During the summer dry season, precipitation is generally low, while δD is enriched

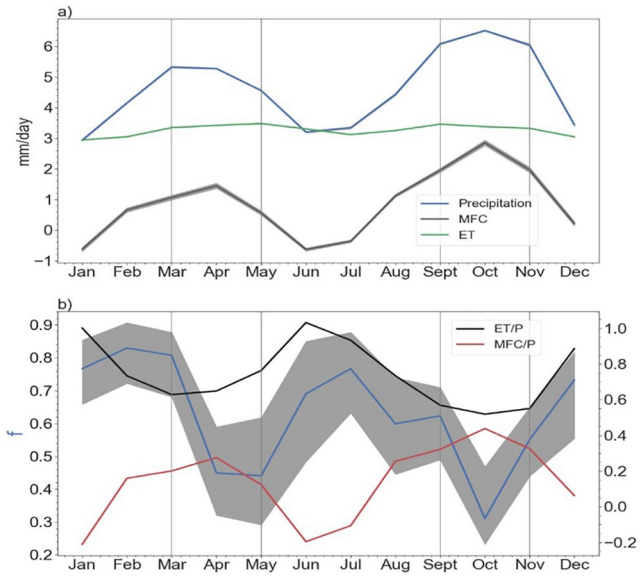

Figure 4. (a) Climatology of Tropical Rainfall Measuring Mission (TRMM) precipitation (P), ERA5 integrated moisture flux convergence (MFC), and Fisher-produced evapotranspiration (ET) averaged within the Congo Basin region. Gray shading is the standard error. In general, the standard error for ET and P was too small to show up on the plots. (b) Climatology of ET/P, MFC/P, and *f*.

compared to the rainy seasons, but lower compared to the winter dry season. Because precipitation is lower, this could indicate that rainout has less impact on depleting δD during the summer dry season and instead it is possible that ocean evaporation advected into the region plays a larger role in contributing to moisture in the summer dry season compared to the winter dry season. During the winter dry season, δD is enriched maximally, despite increased precipitation from January to February. This could indicate that ET is the main contributor to moisture for the winter dry season and the onset of the spring rainy season in February.

In general, f follows a similar seasonal pattern to δD in Figure 3a: f is higher during the two dry seasons in winter and summer and lower during the two rainy seasons in spring and fall (Figure 3b). Maximum f (0.83 ± 0.09) occurs during February, suggesting that increasing vapor from the land areas with high ET is the main reason for increasing free tropospheric specific humidity (q_0) prior to and during the onset of the spring rainy season. In contrast, f is lower during August (0.59 ± 0.15) than during February, suggesting that increasing advected ocean evaporation contributes to the increasing q_0 during the transition to fall rainy season. However, throughout the winter and early spring, f remains above ~ 0.6, meaning that most of the observed δD measurements during those months must come from land. This indicates that ET is the main source of moisture for the dry seasons. As the rainy seasons reach their peaks, f reduces to 0.45 ± 0.13 in mid-spring (April), and 0.31 ± 0.12 in midfall (October). Throughout the rainy seasons, f only remains above ~ 0.6 in March and September. As these are the beginning months of the spring and fall rainy season, respectively, these f values indicate that ET is still an important contributor to moisture for the rainy seasons. But, f and δD both decrease in the next couple of months likely due to a combination of (a) increasing transport from ocean presumably driven by increased latent heating and (b) increasing δD depletion from rainout.

Unfortunately, the δD observations cannot directly quantify the relative contribution of ocean and land sources without further knowledge from other observations. Reanalysis and remotely sensed data, on the other hand, can provide quantitative information on the Congo Basin moisture budget. Due to a lack of observational data, many previous studies have used reanalysis to analyze the moisture sources and dynamics of the Congo Basin. However, monthly reanalysis estimates of tropical precipitation and ET are known to be erroneous due to lack of observational constraints in tropical Africa (e.g., Fekete et al., 2004; Hua et al., 2019). As we do not have independent data sets to validate the current ET datasets and provide the most accurate ET and precipitation data sets over the Congo for this study, we choose to use moisture flux convergence (MFC) from ERA 5 reanalysis as well as precipitation from TRMM, and ET from a MODIS-based product (Fisher et al., 2009) for the purpose of examining the seasonality of the moisture budget (e.g., Shi et al., 2019). We examine the seasonal cycles of the moisture budget components, as well as calculate the fractional contributions of ET and MFC to precipitation, to compare their relative contributions to precipitation in Figure 4.

Figure 4a shows that precipitation varies between 3.0 and 5.4 mm/day over the winter-spring period, and between 3.0 and 6.6 mm/day in summer-fall period, respectively. ET from the MODIS-based data set contributes about 3.0 mm/day of the moisture to atmospheric moisture during winter and summer dry seasons and increases slightly to 3.3 mm/day in spring and fall rainy seasons. The net moisture transport generally contributes much less to the atmospheric moisture than ET: from negative (moisture export) 0.5 mm/day in winter to positive (moisture import) 1.5 mm/day in spring, and from negative 0.5 mm/day in summer to positive 2.6 mm/day in fall. Note that there is a general imbalance of 0.5 mm/day between precipitation estimated by TRMM and the sum of ET and net moisture transport estimated by MODIS and ERA5, although their seasonal variations are consistent.

Figure 4b shows the contributions of ET and MFC to precipitation within our Congo domain, as indicated by ET/P and MFC/P. ET/P shows consistently high values throughout the year and MFC/P is always lower than that of ET/P (e.g., Burnett et al., 2020; Crowhurst et al., 2020). These data support our conclusion that there is a larger relative contribution of ET to the moisture for the spring versus fall rainy seasons. We also compare the seasonal cycle of f to that of ET/P (Figure 4b). f represents the fractional ET contribution from both our Congo domain and upstream regions to the free tropospheric moisture within our Congo domain, whereas ET/P represents the local ET contribution to precipitation all within our Congo domain. In addition, f represents a lower bound of the contribution of land to atmospheric water vapor due to choosing a high δD threshold for moisture from land as well as the potential δD depletion from precipitation. However, we believe it is still useful to compare as their common component is ET and ET/P is widely cited in literature as a local precipitation-recycling indicator. The seasonal variations of f and ET/P can be similar during the dry seasons when they are dominated by the change of local ET as moisture transport from ocean and precipitation are moderate. During the peak rainy seasons, variations of f and ET/P are dominated by a significant increase of precipitation and moisture transport from ocean. However, in the early spring rainy season (February-March), the variations of f and ET/P are distinctively different. This could be for a variety of reasons. For example, it is possible that the difference between f and ET/P originates from scale differences: f is a metric of the relative contribution of ET to atmospheric moisture from anywhere, whereas ET/P represents the fraction of precipitation that originates from ET in the same grid box. ET/P could decrease as the increase in P outpaces the local increase in ET during February-March, but the increase in P could be outpaced by the increase both regional and local ET, as represented by f. Furthermore, the disagreements could be due to the quality of the data. Studies show seasonal ET cycles from models, reanalysis, and other remotely sensed products that vary greatly in their magnitude of seasonality (e.g., Burnett et al., 2020; Crowhurst et al., 2020). The decreased sensitivity of remotely sensed ET during the wet seasons (Fekete et al., 2004; Pan et al., 2020), or the uncertainties of ET estimates based on MODIS in evergreen tropical rainforests (Paca et al., 2019) could lead to underestimates of the seasonal variations of ET.

4.2. Interpretation of These Relative Contributions Based on Spatial Patterns

As discussed previously, the deuterium-based data provides a lower bound estimate on how ET contributes seasonally to atmospheric moisture over the Congo. In this section, we discuss additional evidence based on analysis of moisture flux convergence and winds as well as satellite-based photosynthesis measurements. To examine the role of winds in bringing in moisture to the region, we investigate the spatial patterns of moisture flux convergence (MFC), precipitation, 800–875 hPa averaged wind, δD, and SIF over the Congo Basin for the following months: (a) during the transition month (February) to the spring rainy season, and the peak month of the spring rainy season (April) and (b) during the transition month (August) to the fall rainy season the peak month of the fall rainy season (October).

Figure 5a shows that in February, enriched δD ($\delta D > -75‰$) is concentrated within the Congo Basin, with the exception of enriched values to the northeast where high mountainous ranges penetrate further into the atmospheric boundary layer and push high δD values from the atmospheric boundary layer into the free troposphere. δD is highest in the middle and east of the Congo Basin (20° – 30° E), corresponding with relatively high SIF and rainfall (Figure 5b). This covariation of δD values and SIF indicates that transpiration is one of the main components of ET contributing to atmospheric moisture during this time as photosynthesis co-varies with transpiration (e.g., Boese et al., 2017 and references therein). The increase of rainfall does not contribute to the increase of δD, as it would preferentially remove δD in the atmosphere. The covariance between SIF and rainfall suggests that vegetation photosynthesis also increases with an increase of rainfall.

Furthermore, no winds from either the Atlantic Ocean or Indian Ocean bring depleted δD into the Congo Basin (Figure 5b), and there is little moisture flux convergence the basin (Figure 5a). These conditions all point toward ET being the primary source of moisture in the spring rainy season, generally consistent with Sorí et al. (2017). While March δD values (not shown) remain similar to its distribution in February, δD values in April (Figure 5c), the peak of the boreal spring rainy season, show that enriched δD values occur mostly in the northern part of the basin, which corresponds with relatively higher SIF. However, in general, δD is more depleted than in February. This is likely due to a combination of (a) winds bringing in moisture from the Indian Ocean and (b) the rainout process as described in Section 3, as indicated by high

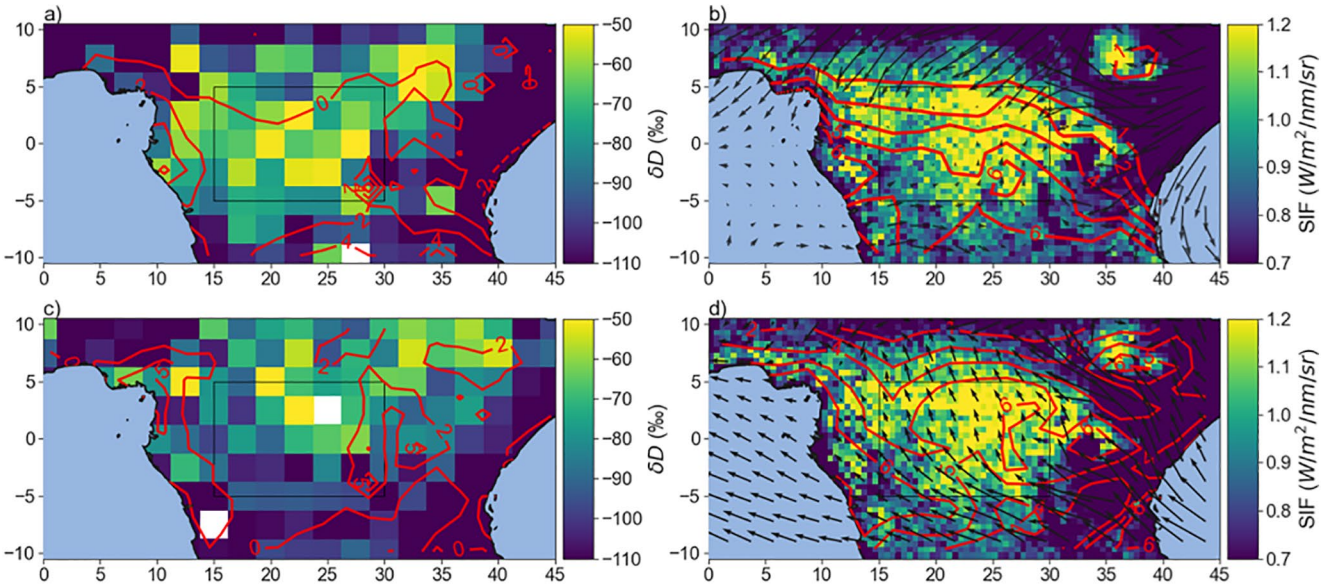

Figure 5. (a) Free tropospheric δD (shaded), integrated moisture flux convergence (contours, units of mm/day) in February. The mean standard error of gridded δD was 13.26‰. White boxes denote the absence of δD measurements for that grid box. (b) solar induced fluorescence (SIF) (shaded), precipitation (contours, units of mm/day), and reanalysis winds averaged over 800–875 hPa (vectors, unit: m/s) in February. (c) Same as (a), but for April. The mean standard error of gridded δD was 12.81‰. (d) Same as (b), but for April.

rainfall within a larger portion of the basin. This does not necessarily mean that the contribution of ET to atmospheric moisture decreases, only that its relative contribution drops as moisture from the ocean or the monsoon region increases. Overall, Figure 5 shows enriched δD, high corresponding SIF, and lack of moisture transport by winds, in February, indicating that ET is the main moisture contributor for the transition to spring rainy season, while in April, the presence of winds from the Indian Ocean combined with depleted δD indicate a higher relative contribution of advected ocean evaporation.

In August (Figure 6a), one month prior to the boreal fall rainy season, δD values are more depleted than in February, with the majority of observations ranging from ~ –100‰ to – 70‰. Enriched δD values in the

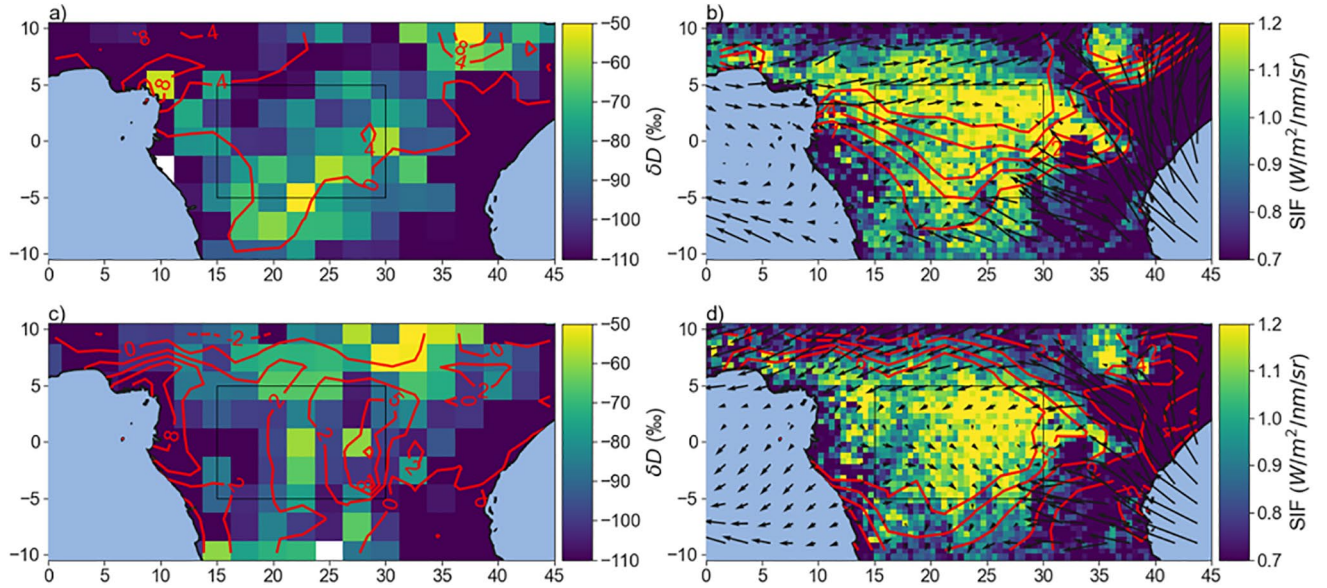

Figure 6. Same as Figure 5 but for August (top panels) and October (bottom panels).

southern part of the basin correspond with relatively high SIF. While the highest SIF is located in the northern part of the basin, δD values there are depleted likely because winds carry moisture from the Atlantic Ocean into that part of the region, which mixes with the enriched δD from plants. In October, during the peak of the boreal fall rainy season (Figure 6d), highest SIF concentrates in the eastern part of the basin, mostly likely as a result of increased precipitation. Since Figure 6d indicates a lack of low-level westerlies reaching the Congo Basin from the Atlantic, moisture is most likely brought in by strong meridional flow related to the African Easterly Jet (AEJ) from areas with mesoscale convective systems (Cook & Vizy, 2016; Pokam et al., 2012). These winds bring depleted δD to the Congo Basin (Figure 6c), which partially offsets the positive influence of ET on δD. Rainfall processes also likely decrease δD compared to δD in August. Overall, in Figure 6, depleted δD values (compared to February) spatially correspond to moisture transport from the Atlantic Ocean in August, while rainout and possible moisture brought in by the AEJ deplete δD over the entire Congo Basin in October.

5. Discussion

Recycling ratios from previous studies indicate significant contributions of ET (greater than 50%) to atmospheric moisture throughout the year (e.g., Nicholson et al., 1997; Risi et al., 2013); however, while it is desirable to compare our assessment of the role of ET in contributing to atmospheric moisture to that suggested by previous studies that calculate continental recycling ratios, a direct comparison is not currently feasible. This is because the recycling rate in literature is mostly defined either as the fractional contribution of ET to precipitation or by local ET versus moisture advected from outside regions, whereas δD is linked to the ratio of water vapor from ET to the total water vapor in the atmosphere (Risi et al., 2013). In addition, δD is influenced by ET both locally and along the path of the air mass, including ET from areas outside the Congo Basin when wind, and thus moisture advection, is strong. Therefore, we can only compare previous studies that quantify the ET contribution to water vapor considered from regions both inside and outside the Congo Basin domain (e.g., Risi et al., 2013; van der Ent et al., 2010; Yoshimura et al., 2004). For example, Risi et al. (2013) used a combined δD observations by TES and a water vapor tagging approach in a climate model. Their result suggests that ET provides more than half of the atmospheric moisture (about 65%) in the winter and summer dry seasons in the Congo region. Our estimates are qualitatively consistent with their result for these two dry seasons, although they suggest that the ET contribution could be somewhat higher than their model values based on comparison with the TES data. Furthermore, Pokam et al. (2012) suggests that ET influences spring rainy season changes more than fall rainy season changes. Our results clarify that this stronger influence in spring is likely because ET is the primary source of atmospheric moisture during the spring rainy season; therefore, changes in ET likely impact rainfall in spring.

Is it possible that the relatively higher ET contribution to atmospheric moisture for spring versus fall is not just due to increased contribution from advected ocean evaporation to atmospheric moisture for the fall rainy season? Previous studies have found a higher ET contribution to the moisture budget during the spring rainy season compared to that of the fall rainy season, which could also help explain why ET contributes more moisture for the spring rainy season. On the other hand, Burnett et al. (2020) calculated basin-scale ET in the Congo using water-balance methods, positing that increased radiation, as well as the availability of soil moisture, can explain increased ET in the spring: Higher direct photosynthetically active radiation (PAR) fractions combined with higher net solar radiation increase water use efficiency, while increased terrestrial water storage increases the amount of water available for transpiration. Crowhurst et al. (2020), using global climate models, also calculated ET over a similar domain and found that it was higher in the spring rainy seasons compared to the fall rainy season. They attributed changes in leaf area index and vapor pressure deficit to changes in transpiration between the spring and fall rainy season.

How does the relative contribution of ET to atmospheric moisture over Congo Basin compare to that over the Amazon basin? δD values are on average more enriched over the Congo Basin than over the Amazon rainforest. In the Congo Basin, δD values are on average –88 ‰ annually, –87 ‰ during the boreal spring rainy season, and the summer dry season, – 94 ‰ during the boreal fall rainy season, and –79 ‰ during the boreal winter dry season (Figure 3a). In contrast, δD values over the Amazon are on average ~ –130 ‰ annually, –139 ‰ during the wet season (October-May), and –126 ‰ during the dry season (June-September). These differences are broadly consistent with a higher recycling rate in the Congo than in the Amazon as

suggested by some studies (e.g., Nicholson et al., 1997; Risi et al., 2013). The recycling rate over the Amazon ranges from about 30% (e.g., Staal et al., 2018) based on reanalysis data to about 50% (Salati et al., 1979) based on isotopic composition of the stream flows. A higher ET contribution to atmospheric moisture in the Congo Basin versus the Amazon basin, as suggested by δD data, is also qualitatively consistent with the ET estimated from water balances using rainfall and runoff data. The annual ET is estimated to contribute to 75%–85% of the annual rainfall in Congo Basin versus 50%–62% in the Amazon basin (Alsdorf et al., 2016; Fernandes et al., 2008; Molion, 1975). Therefore, ET is central in determining the climate variability and change of the water cycle in Congo Basin which has a rainfall regime drier than the Amazon. Our results imply that the loss of rainforests due to land use, biomass burning, and climatic drying in Congo (Bell et al., 2015; Staal et al., 2016) will likely have a greater impact on rainfall in the Congo than in the Amazon basin, especially for the spring rainy season.

6. Conclusions

Most previous studies of the Congo Basin rainy seasons have focused on clarifying the impacts of moisture transport from oceans on rainfall variability and changes. In contrast, the role of vegetation and its modulation from land-use and deforestation have been far less clear due to lack of adequate observations. Using a suite of satellite measurements, including the deuterium content of water vapor and SIF, we show that plant-transpired water, lifted into the free troposphere, is a primary moisture source for the atmosphere during boreal winter (DJF) and summer (JJA). However, both moisture advected from oceans and water transpired from the Congo rainforests are important moisture sources during the rainy seasons (March-May and September-November).

Specifically, the climatology of δD points toward ET being the main initial contributor to atmospheric moisture during February, the transition month to the spring rainy season but less so in August, the transition month to the fall rainy season. f, the fraction of the observational samples for which δD exceeds that of the uppermost land-based mixing model line (Figure 2), is $83\% \pm 9\%$ in February versus $59\% \pm 15\%$ of total water vapor samples in the Congo domain in August. Enriched δD in February corresponds with relatively high SIF and a lack of winds bringing moisture in from the Atlantic Ocean, while relatively depleted δD in August is due to winds bringing in moisture from the Atlantic Ocean and mixing with the enriched δD from areas with high SIF within the Congo Basin. As the rainy season reaches its peak in both spring and fall, δD decreases and the fraction of the observed water vapor samples most likely from ET reduces to $45\% \pm 13\%$ in April and $31\% \pm 12\%$ in October as expected from deep convection and precipitation, and increased moisture transport from the ocean. In general, the climatological seasonal cycles of ET, precipitation and moisture flux convergence (MFC) derived from satellite observations and reanalysis are consistent with the δD results in that both show a higher ET contribution to atmospheric moisture during dry seasons than during the wet seasons. However, neither of these estimates of ET can capture the high ET contribution in the winter/early spring as shown by the δD data.

Our results imply the need to evaluate the possible change of photosynthesis and ET seasonality as a potential contributor to changes to the spring rainy season, in addition to other potential external forcings, such as SSTA, and changes to moisture transport and the African Easterly Jet. For example, observations have shown an earlier than normal onset and demise of the spring rainy season (Jiang et al., 2019; Taylor et al., 2018) over this region due to increased rainfall in February and decreased rainfall in May-June. Furthermore, our results raise several questions: Would the spring rainy season disappear or substantially weaken if ET were substantially reduced by rainforest loss? Are the mechanisms for the onset of spring rainy season significantly different from those of the fall rainy season? What roles do shallow convection versus lower tropospheric circulation play in lifting plant transpired water vapor from the surface to the free troposphere? Why does ET contribute more to the atmospheric moisture in the Congo than in the Amazon basin? Further study is needed to better elucidate these different mechanisms and discover how they might change with climate and land use.

Data Availability Statement

Datasets used are the TES version 6 (v006_Litev01.00) Level 2 HDO and H_2O (https://catalog.data.gov/dataset/tes-aura-l2-hdo-limb-v006) to calculate δD, GOME-2 V26 740 nm SIF estimates (https://avdc.gsfc.nasa.gov/pub/data/satellite/MetOp/GOME_F/), precipitation estimates from the 3B42 TRMM data set (https://disc.gsfc.nasa.gov/datasets/TRMM_3B43_7/summary), water vapor from the V6 AIRS/Aqua L3 data set (https://disc.gsfc.nasa.gov/datasets/AIRS3STM_006/summary?keywords=AIRS%20L3), ERA5 reanalysis products (https://www.ecmwf.int/en/forecasts/datasets/reanalysis-datasets/era5), and "observed" ET from the PT-JPL, Appendix A.6 data set produced by Joshua Fischer (http://josh.yosh.org/).

Acknowledgments
The authors thank Robert Dickinson for very helpful comments. This study was supported by NASA INCA (Grant number NNX16AN12G), FINESST (Grant Number 19-EARTH20-0240), JPL undergraduate summer intern program in 2018, the National Science Foundation (Award No. 1917781), and a Startup fund provided to Rong Fu by the University of California Los Angeles. Part of this research was carried out at the Jet Propulsion Laboratory, California Institute of Technology, under a contract with the National Aeronautics and Space Administration.

References

Alsdorf, D., Beighley, E., Laraque, A., Lee, H., Tshimanga, R., O'Loughlin, F., et al. (2016). Opportunities for hydrologic research in the Congo Basin. *Reviews of Geophysics*, *54*(2), 378–409. https://doi.org/10.1002/2016RG000517

Bailey, A., Blossey, P. N., Noone, D., Nusbaumer, J., & Wood, R. (2017). Detecting shifts in tropical moisture imbalances with satellite-derived isotope ratios in water vapor. *Journal of Geophysical Research: Atmospheres*, *122*(11), 5763–5779. https://doi.org/10.1002/2016JD026222

Balas, N., Nicholson, S. E., & Klotter, D. (2007). The relationship of rainfall variability in West Central Africa to sea-surface temperature fluctuations. *International Journal of Climatology*, *27*(10), 1335–1349. https://doi.org/10.1002/joc.1456

Bell, J. P., Tompkins, A. M., Bouka-Biona, C., & Sanda, I. S. (2015). A process-based investigation into the impact of the Congo Basin deforestation on surface climate. *Journal of Geophysical Research: Atmospheres*, *120*(12), 5721–5739. https://doi.org/10.1002/2014JD022586

Boese, S., Jung, M., Carvalhais, N., & Reichstein, M. (2017). The importance of radiation for semiempirical water-use efficiency models. *Biogeosciences*, *14*(12), 3015–3026. https://doi.org/10.5194/bg-14-3015-2017

Bretherton, C. S., Peters, M. E., & Back, L. E. (2004). Relationships between water vapor path and precipitation over the tropical oceans. *Journal of Climate*, *17*(7), 1517–1528. https://doi.org/10.1175/1520-0442(2004)017<1517:RBWVPA>2.0.CO;2

Brown, D., Worden, J., & Noone, D. (2008). Comparison of atmospheric hydrology over convective continental regions using water vapor isotope measurements from space. *Journal of Geophysical Research*, *113*(D15), D15124. https://doi.org/10.1029/2007JD009676

Burnett, M. W., Quetin, G. R., & Konings, A. G. (2020). Data-driven estimates of evapotranspiration and its controls in the Congo Basin. *Hydrology and Earth System Sciences*, *24*(8), 4189–4211. https://doi.org/10.5194/hess-24-4189-2020

Cook, K. H., & Vizy, E. K. (2016). The Congo Basin Walker circulation: Dynamics and connections to precipitation. *Climate Dynamics*, *47*(3–4), 697–717. https://doi.org/10.1007/s00382-015-2864-y

Crowhurst, D., Dadson, S., Peng, J., & Washington, R. (2020). Contrasting controls on Congo Basin evaporation at the two rainfall peaks. *Climate Dynamics*, *56*(5), 1609–1624. https://doi.org/10.1007/s00382-020-05547-1

Dai, A. (2013). Increasing drought under global warming in observations and models. *Nature Climate Change*, *3*(1), 52–58. https://doi.org/10.1038/nclimate1633

Dee, D. P., Uppala, S. M., Simmons, A. J., Berrisford, P., Poli, P., Kobayashi, S., et al. (2011). The ERA-Interim reanalysis: Configuration and performance of the data assimilation system. *Quarterly Journal of the Royal Meteorological Society*, *137*(656), 553–597. https://doi.org/10.1002/qj.828

Defourny, P., Lamarche, C., Bontemps, S., De Maet, T., Van Bogaert, E., Moreau, I., et al. (2017). *Land cover climate change initiative: Product user guide v2. Issue 2.0*. Retrieved from http://maps.elie.ucl.ac.be/CCI/viewer/download/ESACCI-LC-Ph2-PUGv2_2.0.pdf

Diem, J. E., Ryan, S. J., Hartter, J., & Palace, M. W. (2014). Satellite-based rainfall data reveal a recent drying trend in central equatorial Africa. *Climatic Change*, *126*, 263–272. https://doi.org/10.1007/s10584-014-1217-x

Eltahir, E. A. B., & Bras, R. L. (1996). Precipitation recycling. *Reviews of Geophysics*, *34*(3), 367–378. https://doi.org/10.1029/96RG01927

Fekete, B. M., Vörösmarty, C. J., Roads, J. O., & Willmott, C. J. (2004). Uncertainties in precipitation and their impacts on runoff estimates. *Journal of Climate*, *17*(2), 294–304. https://doi.org/10.1175/1520-0442(2004)017<0294:UIPATI>2.0.CO;2

Fernandes, K., Fu, R., & Betts, A. K. (2008). How well does the ERA40 surface water budget compare to observations in the Amazon River basin? *Journal of Geophysical Research*, *113*(D11), D11117. https://doi.org/10.1029/2007JD009220

Fisher, J. B., Malhi, Y., Bonal, D., Da Rocha, H. R., De Araújo, A. C., Gamo, M., et al. (2009). The land-atmosphere water flux in the tropics. *Global Change Biology*, *15*(11), 2694–2714. https://doi.org/10.1111/j.1365-2486.2008.01813.x

Frankenberg, C., Fisher, J. B., Worden, J., Badgley, G., Saatchi, S. S., Lee, J.-E., et al. (2011). New global observations of the terrestrial carbon cycle from GOSAT: Patterns of plant fluorescence with gross primary productivity. *Geophysical Research Letters*, *38*(17). https://doi.org/10.1029/2011GL048738

Galewsky, J. (2018). Using stable isotopes in water vapor to diagnose relationships between lower-tropospheric stability, mixing, and low-cloud cover near the island of Hawaii. *Geophysical Research Letters*, *45*(1), 297–305. https://doi.org/10.1002/2017GL075770

Galewsky, J., & Hurley, J. V. (2010). An advection-condensation model for subtropical water vapor isotopic ratios. *Journal of Geophysical Research*, *115*(D16), D16116. https://doi.org/10.1029/2009JD013651

Galewsky, J., Steen-Larsen, H. C., Field, R. D., Worden, J., Risi, C., & Schneider, M. (2016). Stable isotopes in atmospheric water vapor and applications to the hydrologic cycle. *Reviews of Geophysics*, *54*(4), 809–865. https://doi.org/10.1002/2015RG000512

Hersbach, H., Bell, B., Berrisford, P., Hirahara, S., Horányi, A., Muñoz-Sabater, J., et al. (2020). The ERA5 global reanalysis. *Quarterly Journal of the Royal Meteorological Society*, *146*(730), 1999–2049. https://doi.org/10.1002/QJ.3803

Hoerling, M., Hurrell, J., Eischeid, J., & Phillips, A. (2006). Detection and attribution of twentieth-century northern and southern African rainfall change. *Journal of Climate*, *19*(16), 3989–4008. https://doi.org/10.1175/JCLI3842.1

Holloway, C. E., & Neelin, J. D. (2009). Moisture vertical structure, column water vapor, and tropical deep convection. *Journal of the Atmospheric Sciences*, *66*(6), 1665–1683. https://doi.org/10.1175/2008JAS2806.1

Hua, W., Zhou, L., Chen, H., Nicholson, S. E., Raghavendra, A., & Jiang, Y. (2016). Possible causes of the Central Equatorial African long-term drought. *Environmental Research Letters*, *11*(12). https://doi.org/10.1088/1748-9326/11/12/124002

Hua, W., Zhou, L., Nicholson, S. E., Chen, H., & Qin, M. (2019). Assessing reanalysis data for understanding rainfall climatology and variability over Central Equatorial Africa. *Climate Dynamics*, *53*(1–2), 651–669. https://doi.org/10.1007/s00382-018-04604-0

Huffman, G. J., Bolvin, D. T., Nelkin, E. J., Wolff, D. B., Adler, R. F., Gu, G., et al. (2007). The TRMM multisatellite precipitation analysis (TMPA): Quasi-global, multiyear, combined-sensor precipitation estimates at fine scales. *Journal of Hydrometeorology*, *8*(1), 38–55. https://doi.org/10.1175/JHM560.1

James, R., Washington, R., Abiodun, B., Kay, G., Mutemi, J., Pokam, W., et al. (2018). Evaluating climate models with an African lens. *Bulletin of the American Meteorological Society*, *99*(2), 313–336. https://doi.org/10.1175/BAMS-D-16-0090.1

Jiang, Y., Zhou, L., Tucker, C. J., Raghavendra, A., Hua, W., Liu, Y. Y., & Joiner, J. (2019). Widespread increase of boreal summer dry season length over the Congo rainforest. *Nature Climate Change*, *9*, 617–622. https://doi.org/10.1038/s41558-019-0512-y

Joiner, J., Guanter, L., Lindstrot, R., Voigt, M., Vasilkov, A. P., Middleton, E. M., et al. (2013). Global monitoring of terrestrial chlorophyll fluorescence from moderate-spectral-resolution near-infrared satellite measurements: Methodology, simulations, and application to GOME-2. *Atmospheric Measurement Techniques*, *6*(10), 2803–2823. https://doi.org/10.5194/amt-6-2803-2013

Lacour, J.-L., Risi, C., Worden, J., Clerbaux, C., & Coheur, P.-F. (2018). Importance of depth and intensity of convection on the isotopic composition of water vapor as seen from IASI and TES δ D observations. *Earth and Planetary Science Letters*, *481*, 387–394. https://doi.org/10.1016/j.epsl.2017.10.048

Levin, N. E., Zipser, E. J., & Ceding, T. E. (2009). Isotopic composition of waters from Ethiopia and Kenya: Insights into moisture sources for eastern Africa. *Journal of Geophysical Research*, *114*(23). https://doi.org/10.1029/2009JD012166

Majoube, M. (1971). Fractionnement en oxygène 18 et en deutérium entre l'eau et sa vapeur. *Journal de Chimie Physique*, *68*, 1423–1436. https://doi.org/10.1051/jcp/1971681423

Mayer, A. L., & Khalyani, A. H. (2011). Grass trumps trees with fire. *Science*, *334*, 188–189. https://doi.org/10.1126/science.1213908

Molion, L. C. B. (1975). *A climatonomic study of the energy and moisture fluxes of the Amazonas Basin with considerations of deforestation effects*. The University Of Wisconsin - Madison thesis.

Moore, M., Kuang, Z., & Blossey, P. N. (2014). A moisture budget perspective of the amount effect. *Geophysical Research Letters*, *41*(4), 1329–1335. https://doi.org/10.1002/2013GL058302

Munier, S., & Aires, F. (2018). A new global method of satellite dataset merging and quality characterization constrained by the terrestrial water budget. *Remote Sensing of Environment*, *205*, 119–130. https://doi.org/10.1016/j.rse.2017.11.008

Nicholson, S. E. (2018). The ITCZ and the seasonal cycle over equatorial Africa. *Bulletin of the American Meteorological Society*, *99*(2), 337–348. https://doi.org/10.1175/BAMS-D-16-0287.1

Nicholson, S. E., & Dezfuli, A. K. (2013). The relationship of rainfall variability in western equatorial Africa to the tropical oceans and atmospheric circulation. Part I: The boreal spring. *Journal of Climate*, *26*(1), 45–65. https://doi.org/10.1175/JCLI-D-11-00653.1

Nicholson, S. E., Kim, J., Ba, M. B., & Lare, A. R. (1997). The mean surface water balance over Africa and its interannual variability. *Journal of Climate*, *10*(12), 2981–3002. https://doi.org/10.1175/1520-0442(1997)010<2981:TMSWBO>2.0.CO;2

Nlend, B., Celle-Jeanton, H., Risi, C., Pohl, B., Huneau, F., Ngo Boum-Nkot, S., et al. (2020). Identification of processes that control the stable isotope composition of rainwater in the humid tropical West-Central Africa. *Journal of Hydrology*, *584*, 124650. https://doi.org/10.1016/j.jhydrol.2020.124650

Noone, D. (2012). Pairing measurements of the water vapor isotope ratio with humidity to deduce atmospheric moistening and dehydration in the tropical midtroposphere. *Journal of Climate*, *25*(13), 4476–4494. https://doi.org/10.1175/JCLI-D-11-00582.1

Paca, V. H. D. M., Espinoza-Dávalos, G. E., Hessels, T. M., Moreira, D. M., Comair, G. F., & Bastiaanssen, W. G. M. (2019). The spatial variability of actual evapotranspiration across the Amazon River Basin based on remote sensing products validated with flux towers. *Ecological Processes*, *8*(1), 1–20. https://doi.org/10.1186/S13717-019-0158-8

Pan, S., Pan, N., Tian, H., Friedlingstein, P., Sitch, S., Shi, H., et al. (2020). Evaluation of global terrestrial evapotranspiration using state-of-the-art approaches in remote sensing, machine learning and land surface modeling. *Hydrology and Earth System Sciences*, *24*(3), 1485–1509. https://doi.org/10.5194/hess-24-1485-2020

Pokam, W. M., Bain, C. L., Chadwick, R. S., Graham, R., Sonwa, D. J., & Kamga, F. M. (2014). Identification of processes driving low-level westerlies in West Equatorial Africa. *Journal of Climate*, *27*(11), 4245–4262. https://doi.org/10.1175/JCLI-D-13-00490.1

Pokam, W. M., Djiotang, L. A. T., & Mkankam, F. K. (2012). Atmospheric water vapor transport and recycling in Equatorial Central Africa through NCEP/NCAR reanalysis data. *Climate Dynamics*, *38*(9–10), 1715–1729. https://doi.org/10.1007/s00382-011-1242-7

Rauniyar, S. P., Protat, A., & Kanamori, H. (2017). Uncertainties in TRMM-Era multisatellite-based tropical rainfall estimates over the Maritime Continent. *Earth and Space Science*, *4*(5), 275–302. https://doi.org/10.1002/2017EA000279

Reager, J. T., Gardner, A. S., Famiglietti, J. S., Wiese, D. N., Eicker, A., & Lo, M. H. (2016). A decade of sea level rise slowed by climate-driven hydrology. *Science*, *351*(6274), 699–703. https://doi.org/10.1126/science.aad8386

Risi, C., Bony, S., Vimeux, F., Frankenberg, C., Noone, D., & Worden, J. (2010). Understanding the Sahelian water budget through the isotopic composition of water vapor and precipitation. *Journal of Geophysical Research*, *115*(D24). https://doi.org/10.1029/2010JD014690

Risi, C., Muller, C., & Blossey, P. (2020). What controls the water vapor isotopic composition near the surface of tropical oceans? Results from an analytical model constrained by large-eddy simulations. *Journal of Advances in Modeling Earth Systems*, *12*(8). https://doi.org/10.1029/2020MS002106

Risi, C., Noone, D., Frankenberg, C., & Worden, J. (2013). Role of continental recycling in intraseasonal variations of continental moisture as deduced from model simulations and water vapor isotopic measurements. *Water Resources Research*, *49*(7), 4136–4156. https://doi.org/10.1002/wrcr.20312

Salati, E., Dall'Olio, A., Matsui, E., & Gat, J. R. (1979). Recycling of water in the Amazon Basin: An isotopic study. *Water Resources Research*, *15*(5), 1250–1258. https://doi.org/10.1029/WR015i005p01250

Samba, G., & Nganga, D. (2012). Rainfall variability in Congo-Brazzaville: 1932-2007. *International Journal of Climatology*, *32*(6), 854–873. https://doi.org/10.1002/joc.2311

Samuels-Crow, K. E., Galewsky, J., Sharp, Z. D., & Dennis, K. J. (2014). Deuterium excess in subtropical free troposphere water vapor: Continuous measurements from the Chajnantor Plateau, northern Chile. *Geophysical Research Letters*, *41*(23), 8652–8659. https://doi.org/10.1002/2014GL062302

Schiro, K. A., Ahmed, F., Giangrande, S. E., & David Neelin, J. (2018). GoAmazon2014/5 campaign points to deep-inflow approach to deep convection across scales. *Proceedings of the National Academy of Sciences of the USA*, *115*(18), 4577–4582. https://doi.org/10.1073/pnas.1719842115

Shi, M., Liu, J., Worden, J. R., Bloom, A. A., Wong, S., & Fu, R. (2019). The 2005 Amazon drought legacy effect delayed the 2006 wet season onset. *Geophysical Research Letters*, *46*(15), 9082–9090. https://doi.org/10.1029/2019GL083776

Sobel, A. H., Yuter, S. E., Bretherton, C. S., & Kiladis, G. N. (2004). Large-scale meteorology and deep convection during TRMM KWAJEX*. *Monthly Weather Review*, *132*(2), 422–444. https://doi.org/10.1175/1520-0493(2004)132<0422:LMADCD>2.0.CO;2

Sorí, R., Nieto, R., Vicente-Serrano, S. M., Drumond, A., & Gimeno, L. (2017). A Lagrangian perspective of the hydrological cycle in the Congo River basin. *Earth System Dynamics*, *8*(3), 653–675. https://doi.org/10.5194/esd-8-653-2017

Staal, A., Dekker, S. C., Xu, C., & van Nes, E. H. (2016). Bistability, spatial interaction, and the distribution of tropical forests and Savannas. *Ecosystems*, *19*(6), 1080–1091. https://doi.org/10.1007/s10021-016-0011-1

Staal, A., Tuinenburg, O. A., Bosmans, J. H. C., Holmgren, M., Van Nes, E. H., Scheffer, M., et al. (2018). Forest-rainfall cascades buffer against drought across the Amazon. *Nature Climate Change*, *8*(6), 539–543. https://doi.org/10.1038/s41558-018-0177-y

Staver, A. C., Archibald, S., & Levin, S. A. (2011). The global extent and determinants of savanna and forest as alternative biome states. *Science*, *334*(6053), 230–232. https://doi.org/10.1126/science.1210465

Tamoffo, A. T., Moufouma-Okia, W., Dosio, A., James, R., Pokam, W. M., Vondou, D. A., et al. (2019). Process-oriented assessment of RCA4 regional climate model projections over the Congo Basin under 1.5°C and 2°C global warming levels: Influence of regional moisture fluxes. *Climate Dynamics*, *53*(3–4), 1911–1935. https://doi.org/10.1007/s00382-019-04751-y

Taylor, C. M., Fink, A. H., Klein, C., Parker, D. J., Guichard, F., Harris, P. P., & Knapp, K. R. (2018). Earlier seasonal onset of intense mesoscale convective systems in the Congo Basin since 1999. *Geophysical Research Letters*, *45*(24), 13458–13467. https://doi.org/10.1029/2018GL080516

Thorne, P. W., & Vose, R. S. (2010). Reanalyses suitable for characterizing long-term trends. *Bulletin of the American Meteorological Society*, *91*(3), 353–361. https://doi.org/10.1175/2009bams2858.1

Tremoy, G., Vimeux, F., Soumana, S., Souley, I., Risi, C., Favreau, G., & Oï, M. (2014). Clustering mesoscale convective systems with laser-based water vapor $\delta^{18}O$ monitoring in Niamey (Niger). *Journal of Geophysical Research*, *119*(9), 5079–5103. https://doi.org/10.1002/2013JD020968

Trenberth, K. E. (1999). Atmospheric moisture recycling: Role of advection and local evaporation. *Journal of Climate*, *12*(5 II), 1368–1381. https://doi.org/10.1175/1520-0442(1999)012<1368:amrroa>2.0.co;2

van der Ent, R. J., Savenije, H. H. G., Schaefli, B., & Steele-Dunne, S. C. (2010). Origin and fate of atmospheric moisture over continents. *Water Resources Research*, *46*(9). https://doi.org/10.1029/2010WR009127

Washington, R., James, R., Pearce, H., Pokam, W. M., & Moufouma-Okia, W. (2013). Congo basin rainfall climatology: Can we believe the climate models? *Philosophical Transactions of the Royal Society B: Biological Sciences*, *368*(1625). https://doi.org/10.1098/rstb.2012.0296

Worden, J., Kulawik, S., Frankenberg, C., Payne, V., Bowman, K., Cady-Peirara, K., et al. (2012). Profiles of CH_4, HDO, H_2O, and N_2O with improved lower tropospheric vertical resolution from Aura TES radiances. *Atmospheric Measurement Techniques*, *5*(2), 397–411. https://doi.org/10.5194/amt-5-397-2012

Worden, J., Noone, D., Bowman, K., Beer, R., Eldering, A., Fisher, B., et al. (2007). Importance of rain evaporation and continental convection in the tropical water cycle. *Nature*, *445*(7127), 528–532. https://doi.org/10.1038/nature05508

Wright, J. S., Fu, R., Worden, J. R., Chakraborty, S., Clinton, N. E., Risi, C., et al. (2017). Rainforest-initiated wet season onset over the southern Amazon. *Proceedings of the National Academy of Sciences of the USA*, *114*(32), 8481–8486. https://doi.org/10.1073/pnas.1621516114

Yoshimura, K., Oki, T., Ohte, N., & Kanae, S. (2004). Colored moisture analysis estimates of variations in 1998 Asian monsoon water sources. *Journal of the Meteorological Society of Japan*, *82*, 1315–1329. https://doi.org/10.2151/jmsj.2004.1315

Zhou, L., Tian, Y., Myneni, R. B., Ciais, P., Saatchi, S., Liu, Y. Y., et al. (2014). Widespread decline of Congo rainforest greenness in the past decade. *Nature*, *508*(7498), 86–90. https://doi.org/10.1038/nature13265